# X-ray Structure of the Polyaniline Derivative Poly(*o*-toluidine): The Structural Origin of Charge Localization

**M. E. Józefowicz[†] and A. J. Epstein***

*Departments of Physics and Chemistry, The Ohio State University, Columbus, Ohio 43210-1106*

**J. P. Pouget**

*Laboratoire de Physique des Solides and LURE, Université Paris-Sud, 91405 Orsay, France*

**J. G. Masters, A. Ray,[‡] and A. G. MacDiarmid**

*Department of Chemistry, University of Pennsylvania, Philadelphia, Pennsylvania 19104*

*Received March 14, 1991; Revised Manuscript Received June 18, 1991*

ABSTRACT: We investigate the structural features of the polyaniline derivative poly(*o*-toluidine)(POT). In the base form POT is amorphous, with an X-ray diffraction pattern similar to that of emeraldine base EB-I. We estimate from the position of the broad peaks in the amorphous pattern that the interchain spacing is larger in POT-EB than in EB-I. POT hydrochloride is partially crystalline with a diffraction pattern resembling that of emeraldine hydrochloride ES-I. Analysis of the data shows that the crystalline part of POT hydrochloride adopts the ES-I-like structure, with increased zigzag angle of the polymer chain and larger interchain spacing, together with an increased disorder, possibly due to defects in the stacking of polymer chains caused by the bulky $CH_3$ groups. Structure and percent crystallinity evolve with doping level in the same way as in the EB-I–ES-I emeraldine system. These structural results correlate with difference in the electronic properties of POT-ES as compared with ES-I. In particular, the $10^3$ decrease in room temperature conductivity of POT-ES compared to ES-I and concomitant localization of conduction electrons in POT-ES as compared with PAN-ES are attributed to the increased separation and decreased coherence between polymer chains leading to quasi-one-dimensional localization of conduction electrons.

## 1. Introduction

The polyaniline family of polymers has become a prototype system for study of control of electronic phenomena due to the ease of its processability and ready derivatization.[1-3] Recent studies have shown a 2 order of magnitude increase in conductivity of emeraldine hydrochloride (PAN-ES) with increased orientation and crystallinity.[4,5] In contrast, extensive experiments on the methyl derivative of polyaniline, poly(*o*-toluidine) (POT) (Figure 1), have demonstrated that its hydrochloride salt (POT-ES) has the same electronic structure as PAN-ES yet dramatically reduced conductivity.[6] The origin of these contrasting phenomena has been proposed[6] as due to increased conduction electron localization in POT-ES as compared to PAN-ES caused by an increased interchain separation and reduced interchain order. The roles of intrachain and interchain spatial coherences have been suggested as central to the formation of the metallic state in polymers.[6-9] Detailed studies of the evolution of the structures of polyanilines are therefore essential.

The crystal structure of the parent polyaniline has received substantial attention.[10-13] It was shown that there were two distinct structural classes for emeraldine.[11,12] Class I materials consisted of those prepared from solution in the conducting salt form. They have ES-I crystal structure in their ordered regions. When dedoped, they form essentially amorphous EB-I. Class II materials consist of those prepared in the insulating base form. They have the EB-II crystal structure in their ordered regions and, when doped, have the ES-II crystal structure. A detailed description of the differences in the ES-I and ES-II crystal structures has been reported earlier.[12]

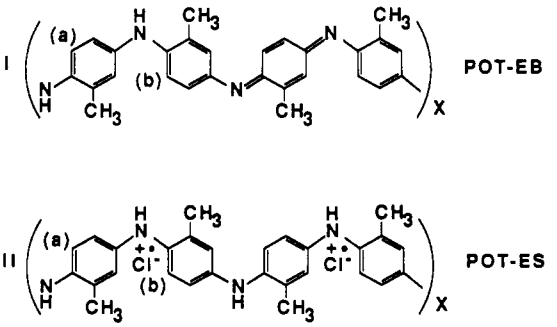


**Figure 1.** Schematic formulas of (I) POT-EB and (II) POT-ES. Due to ring torsional motion about the N–N axis, there are two possible locations for the methyl group (a and b) on each benzene ring.

We report here the results of a detailed structural study of poly(*o*-toluidine). We find that POT is very similar to Class I of emeraldine in the evolution of its structure from nearly amorphous base (POT-EB) to partially crystalline HCl salt (POT-ES) on equilibration with HCl solution of appropriate pH. We have been unsuccessful at preparing a POT analogue of EB-II- and ES-II-like phases. There are significant differences between POT-EB and -ES and PAN-EB-I and -ES-I as well. These include an average ~4% larger interchain spacing and reduced spatial interchain coherence. These results support the thesis that the dramatic differences in transport phenomena between POT-ES and PAN-ES are due to increased localization of conduction electrons caused by reduced interchain overlap and spatial coherence.

## 2. Experimental Methods

Poly(*o*-toluidine) was synthesized in the HCl salt form (POT-ES) according to the standard procedure,[15] which is very much

[†] Chemical Physics Program, The Ohio State University, Columbus, OH 43210-1106.

[‡] Present address: Alchemi Research Centre, Naharashtra, India.

0024-9297/91/2224-5863$02.50/0 

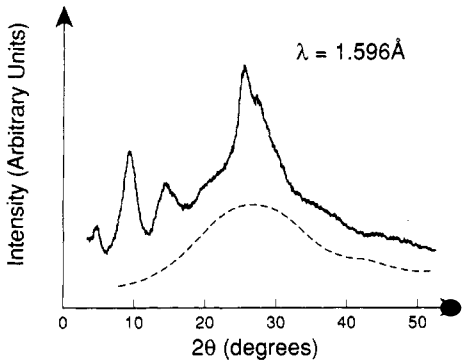


**Figure 2.** X-ray Debye–Scherrer pattern from "as-prepared" poly(*o*-toluidine hydrochloride), taken at LURE (λ = 1.596 Å). Dashed line shows contribution from glass sample holder.

**Table I**
***d* Spacing, Coherence Length *L*, and Intensity Corresponding to Crystalline Reflections of POT-ES "As Prepared" and Redoped to [Cl]/[N] ~ 0.5[a]**

| *d* spacing (*L*), Å | | | |
|---|---|---|---|
| POT-ES as prepared | POT-ES redoped | ES-I (from ref 12) | (*hkl*) |
| ~20 (60) w | | | |
| 9.95 (40) s | 9.85 (35) s | 9.57 (45) s | (001) |
| 6.5 (35) m | 6.4 (35) m | 5.94 (35) s | (010) |
| ~4.7* | ~4.7* | 4.26 (35) s | (100) |
| 3.61 (40) s | 3.61 (35) s | 3.51 (70) vs | (110) |
| 3.38 w | 3.36 w | 3.28 m | (111) |
| ~3.25 vs | 3.23 vw | 2.98 w | (020) |
| ~3.03 vw | ~3.03 vw | 2.85 vw | (021) |
| ~2.45 vw | ~2.42 vw | 2.47 vw | |
| | | 2.34 vw | |
| ~2.10 vw | ~2.08 vw | 2.10 vw | |
| | | 1.72 vw | |

[a] For comparison, the ES-I data of ref 12 and (*hkl*) indexing with a pseudoorthorhombic structure are given. The *d* spacing of asymmetric reflections (*) corresponds to the low-2θ edge of scattering.

similar to the emeraldine synthesis method.[3] It was then converted to the base (POT-EB) form by washing with 0.1 M $NH_4OH$ solution. The base form was subsequently doped by equilibrating POT-EB powder with aqueous solutions of HCl of various concentration. The maximal doping level of [Cl]/[N] = 0.5 was attained by stirring POT-EB with 2.5 M HCl. The [Cl]/[N] ratios (i.e., doping levels) of doped samples were determined by elemental analyses. Attempts at preparing partially crystalline POT-EB from *N*-methyl-2-pyrrolidone (analogous to preparation of partially crystalline EB-II) were unsuccessful.

As in our earlier studies of the emeraldine system,[11,12,14] X-ray data were collected on photographic films fixed in a cylindrical camera with the powder sample placed in a sealed Lindemann glass capillary in the center of the evacuated chamber. X-ray patterns were taken with monochromatized Cu Kα (λ = 1.542 Å) radiation. Additional data were also obtained with higher resolution X-ray synchrotron radiation (λ = 1.596 Å) at station D-16 at LURE (Orsay). X-ray films were read in the equatorial plane with a Joyce-Loeble microdensitometer.

## 3. Experimental Results

A Debye–Scherrer pattern of "as-prepared" POT-ES is shown in Figure 2. This spectrum was taken with synchrotron radiation, λ = 1.596 Å. It exhibits well-defined reflections characteristic of crystalline order on top of a broad scattering feature from amorphous regions of the sample and the Lindemann glass sample holder. An asymmetric reflection with a long tail toward larger values of 2θ can also be seen at ca. 2θ ~ 19°. The *d* spacings calculated from the angular positions of the reflections and the edge of this asymmetric scattering for both "as-prepared" POT-ES and POT-ES after dedoping and redoping to [Cl]/[N] ~ 0.5 are given in Table I. For

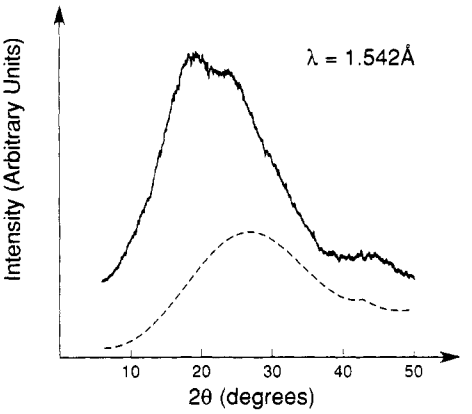


**Figure 3.** X-ray Debye–Scherrer pattern from poly(*o*-toluidine) base (λ = 1.542 Å). Dashed line shows contribution from glass sample holder.

**Table II**
***d* Spacing Corresponding to Broad Peaks and a Bump (~) Observed in the X-ray Patterns of POT-EB and EB-I[a]**

| *d* spacing, Å | | |
|---|---|---|
| POT-EB | EB-I | (*hkl*) |
| 4.75 | 4.45 | (110) |
| 3.9 | ~3.75 | (200) |
| ~3.0 | 2.95 | (020) |
| 2.05 | 2.02 | |

[a] The (*hkl*) indexing refers to the EB-II structure defined in ref 12.

comparison purposes, the *d* spacings obtained for partially crystalline emeraldine HCl salt ES-I ([Cl]/[N] ~ 0.5)[12] are also presented in that table.

The rings are broader than the experimental resolution of the apparatus (fwhm Δ(2θ) ≈ 0.05° for the X-ray synchrotron data), and from reflection broadening Δ(2θ) the coherence length of the crystalline order in the sample *L* is calculated, using the Scherrer formula:[16]

$$L = \frac{0.9\lambda}{\Delta(2\theta)\cos\theta} \quad (1)$$

The *L* values are also given in Table I. They are of the order of 40 Å.

The sharp, crystalline rings of POT-ES disappear when the sample is dedoped, that is, converted to the base form, POT-EB. A typical Debye–Scherrer pattern of POT-EB is shown in Figure 3. It was taken with Cu Kα radiation (λ = 1.542 Å). It consists mainly of one broad reflection centered around 2θ ~ 19° (*d* ~ 4.75 Å) and weaker broad features at 2θ ~ 23° (*d* ~ 3.9 Å) and 2θ ~ 44° (*d* ~ 2.05 Å). There can also be seen a small bump at 2θ ~ 30° (*d* ~ 3 Å). For reference, the scattering from an empty glass capillary is indicated. These data are summarized in Table II, together with values obtained from emeraldine base EB-I for comparison.

POT-EB when redoped with HCl becomes partially crystalline again, with continuous evolution of the X-ray pattern with doping level. Figure 4 shows Debye–Scherrer patterns for POT samples with doping levels from 0.04 to 0.5. Data were taken with Cu Kα radiation (λ = 1.542 Å). Reflections characteristic of crystalline order emerge gradually as the crystallinity of the sample increases from ~0% for base sample to ~40–50% for the fully doped sample. Their *d* spacings shift slightly with the increased doping level, as can be seen clearly in Figure 5. In Figure 4 it can also be seen how, upon doping, the broad reflection in POT-EB, corresponding to *d* ~ 4.75 Å (2θ ~ 19°),

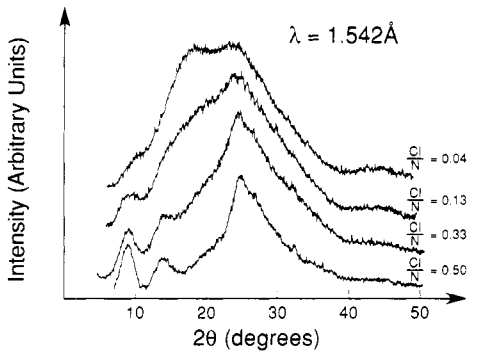


**Figure 4.** Set of microdensitometer readings of X-ray Debye–Scherrer patterns showing the continuous evolution from POT-EB to POT-ES as a function of the [Cl]/[N] ratio (λ = 1.542 Å). The various tracings are not scaled to each other.

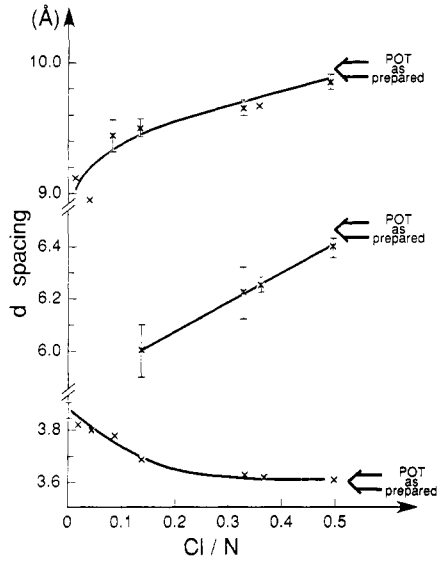


**Figure 5.** Variation of the $d$ spacing of the (001), (010), and (110) reflections (from top to bottom) of POT-ES as a function of the doping level ([Cl]/[N] ratio).

transforms into the asymmetric one at about the same angle in POT-ES.

Diffractometer tracings of as-prepared POT-ES (Figure 2) and dedoped and subsequently redoped POT-ES (Figure 4) are almost identical, showing that there is no significant degradation of the crystalline order in POT-ES upon this dedoping–doping cycle. However, the long $d$-spacing reflection at ~20 Å ($2\theta \sim 4.6°$, Figure 2) has disappeared.

## 4. Discussion of Structural Data

X-ray scattering patterns and their evolution with the doping level of the POT are remarkably similar to that of the EB-I–ES-I system of polyaniline–emeraldine.

**4.1. Poly(*o*-toluidine) Base.** We start our analysis with the quasi-amorphous base form. When the positions of the broad features of POT-EB are compared with data for EB-I (Table II), it can be seen that there is an increase of $d$ spacing from EB-I to POT-EB, but general features of scattering patterns are similar (see Figure 3 in ref 12). We can conclude therefore that the local chain array is similar in both materials.

If we assume that the peaks in the quasi-amorphous spectra of POT-EB correspond to fundamental distances $d_{110}$, $d_{200}$, and $d_{020}$ (by analogy to EB-II), we can calculate approximate interchain lateral distances of $a \sim 7.8$ Å and $b \sim 6.0$ Å, which yields a cross-sectional area for two chains of $A = ab = 47$ Å$^2$. This value can be compared to 44 Å$^2$ in EB-I and EB-II.[12] This represents ~6% increase in $A$ or ~3% increase in the average POT-EB interchain distance with respect to EB. This increase is probably due to the bulky $CH_3$ groups in POT.

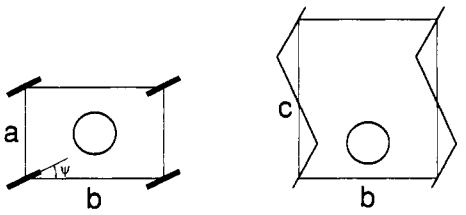


**Figure 6.** Projection along the chain axis and side view of the ES-I pseudoorthorhombic unit cell (from ref 12). Black rectangles on the left drawing represent projections of polymer chains on the $(a,b)$ plane. Zigzags on the right drawing represent schematic view of the polymer chain. Circles denote $Cl^-$ ion.

**4.2. Poly(*o*-toluidine hydrochloride).** The main peaks in the Debye–Scherrer pattern of "as-prepared" POT-ES (Table I) can be indexed with the ES-I-like pseudoorthorhombic cell, shown in Figure 6. However, there is one additional reflection at $d \sim 20$ Å which represents a doubling of the chain axis periodicity. The $c$ parameter, corresponding to one zigzag period of the POT chain, is 9.9 Å. Comparing with $c = 9.6$ Å for ES-I, we conclude that the C–N–C angle of POT-ES is larger. This increase is likely due to steric interactions between hydrogen and methyl groups of neighboring benzene rings. It is noted that the ~20-Å reflection disappears upon dedoping and subsequent redoping. This suggests that this in-chain superlattice periodicity, which is lost upon dedoping and not regained upon redoping, could be due to the long-range order in the methyl group orientation being destroyed in this process.

The interchain order is not as well defined in POT-ES as compared with ES-I. An asymmetric reflection is visible where the (100) peak is anticipated. Such a feature could be explained by a broadening of the (100) reflection in directions perpendicular to $a^*$. In contrast, the (010) and (110) reflections remain clearly defined. However, the (110) reflection is significantly broader when compared with the equivalent one in ES-I. The (010) reflection is not significantly broadened. This means that there is probably a distribution of $a^*$ direction in the diffraction pattern, which is more likely due to shear displacements (probably along $a$) of neighboring $(a,c)$ planes of polymer chains in the ES-I-type structure (see Figure 6). This could be caused by disorder in the placement of $Cl^-$ ions due to some randomness in the position of the methyl groups caused by ring flips. When $d_{010}$ and $d_{110}$ distances of redoped POT-ES and ES-I are compared (Table I), we notice that, as in the base form, the average interchain spacing is larger in POT-ES by ca. 5%.

Apart from the resemblance of the Debye–Scherrer patterns of "as-prepared" ES-I and POT-ES, perhaps the strongest argument for the similarity of their structures is somewhat parallel evolution of their X-ray patterns (Figure 4) and $d$ spacings (Figure 5) with doping level. Figures 4 and 5 can be compared with Figures 4 and 5, respectively, in ref 12. In both materials the $d_{001}$ and $d_{010}$ distances increase with increasing doping level whereas $d_{110}$ decreases. However, while the $d$ spacings of POT-ES vary for the entire [Cl]/[N] range, it was noticed previously[12] that those of ES-I saturate above $x_c \sim 0.2$–0.3.

## 5. Implications for Electronic Phenomena

The structure of the POT-EB–POT-ES system is very close to that of the EB-I–ES-I system. This similarity

makes possible meaningful comparisons of electronic properties between the two. In particular, the increase of the electron localization in POT-ES[6] can be explained by the increase of the interchain spacing and of the interchain disorder reducing the rate of interchain electronic transfer and by the increase of intrachain disorder reducing the in-chain scattering time. The change of parameters is due to the presence of the bulky $CH_3$ groups, and the disorder is certainly caused by some randomness in their placement. Due to this last feature correlated disorder in the ring tilt angle and in the position of the $Cl^-$ ions will also be present.

As discussed in the Introduction, though the electronic structures of POT-ES and PAN-ES appear to be nearly identical, their transport properties are dramatically different, with POT-ES having one-dimensional localization[6] and PAN-ES showing features of three-dimensional delocalization.[17] The direct similarity of the ES-I and POT-ES structures allows conclusions to be drawn concerning the criteria for truly metallic polymers. The POT-ES structure differs from that of PAN-ES-I only in terms of a $\sim 5\%$ increased interchain separation and reduced interchain order. This lends strong support for the critical role of the relative size of the interchain conduction electron transition rate as compared with intrachain scattering rate. The improved order and decreased interchain separation of PAN-ES-I with respect to POT-ES are sufficient to take the former polymer to the edge of three-dimensional delocalization within crystalline regions while POT-ES remains one-dimensionally localized. It is noted that similar criteria for three-dimensional delocalization to achieve the highly conducting metallic state apply to other polymers including polyacetylene, where recent magnetoresistance studies[18] demonstrate that the conduction electrons are only weakly localized. It was also proposed[19] that, correlated with simultaneous changes of $d$ spacings and transverse diffusion coefficient of the carriers with $x$, ES-I undergoes a localization–delocalization electronic transition at about $x_c$.

## 6. Conclusions

The POT-EB–POT-ES system is structurally similar to EB-I–ES-I. This similarity makes possible meaningful comparisons of transport and other properties.[6,17] In particular, the increased electron localization in POT-ES can be explained by increased interchain spacing and increased interchain disorder in poly(*o*-toluidine).

**Acknowledgment.** This work was supported in part by the Defense Advanced Research Project Agency through a contract monitored by the U.S. Office of Naval Research. Laboratoire de Physique des Solides, Laboratoire No. 2, is affiliated with the Centre National de la Recherche Scientifique.

## References and Notes

(1) See, for example: Proceedings of International Conferences on Science and Technology of Synthetic Metals: Tubingen, Germany, Sept 2–8, 1990 (*Synth. Met.* **1991**, *41–43*); Santa Fe, NM, June 27 to July 2, 1988 (*Synth. Met.* **1989**, *27–29*).
(2) Epstein, A. J.; MacDiarmid, A. G. *Mater. Res. Soc. Symp. Proc.* **1990**, *173*, 293.
(3) MacDiarmid, A. G.; Epstein, A. J. *J. Chem. Soc., Faraday Discuss.* **1989**, *88*, 317.
(4) Cromack, K. R.; Józefowicz, M. E.; Ginder, J. M.; Epstein, A. J.; McCall, R. P.; Du, G.; Leng, J. M.; Kim, K.; Li, C.; Wang, Z. H.; Druy, M. A.; Glatkowski, P. J.; Scherr, E. M.; MacDiarmid, A. G. *Macromolecules* **1991**, *24*, 4157.
(5) Scherr, E. M.; MacDiarmid, A. G.; Manohar, S. K.; Masters, J. G.; Sun, Y.; Tang, X.; Druy, M. A.; Glatkowski, P. J.; Cajibe, V.; Fischer, J. E.; Cromack, K. R.; Józefowicz, M. E.; Ginder, J. M.; McCall, R. P.; Epstein, A. J. *Synth. Met.* **1991**; *41*, 735.
(6) Wang, Z. H.; Javadi, H. H. S.; Ray, A.; MacDiarmid, A. G.; Epstein, A. J. *Phys. Rev. B* **1990**, *42*, 5411. Wang, Z. H.; Ray, A.; MacDiarmid, A. G.; Epstein, A. J. *Phys. Rev. B* **1991**, *43*, 4373.
(7) Gogolin, A. A. *Phys. Rep.* **1982**, *1*, 1; **1988**, *5*, 269.
(8) Firsov, Y. A. In *Localization and Metal–Insulator Transitions*; Fritzche, H., Adler, D., Eds.; Plenum Press: New York, 1955; p 477.
(9) Kivelson, S.; Heeger, A. J. *Synth. Met.* **1988**, *22*, 371.
(10) Fosong, W.; Jinsong, T.; Lixiang, W.; Hongfang, Z.; Zhishen, M. *Mol. Cryst. Liq. Cryst.* **1988**, *160*, 175.
(11) Józefowicz, M. E.; Laversanne, R.; Javadi, H. H. S.; Epstein, A. J.; Pouget, J. P.; Tang, X.; MacDiarmid, A. G. *Phys. Rev. B* **1989**, *39*, 12958.
(12) Pouget, J. P.; Józefowicz, M. E.; Epstein, A. J.; Tang, X.; MacDiarmid, A. G. *Macromolecules* **1991**, *24*, 779.
(13) Moon, Y. B.; Cao, Y.; Smith, P.; Heeger, A. J. *Polym. Commun.* **1989**, *30*, 196.
(14) Józefowicz, M. E.; Epstein, A. J.; Pouget, J.-P.; Masters, J. G.; Ray, A.; Sun, Y.; Tang, X.; MacDiarmid, A. G. *Synth. Met.* **1991**, *41*, 723.
(15) Wei, Y.; Focke, W. W.; Wnek, G. E.; Ray, A.; MacDiarmid, A. G. *J. Phys. Chem.* **1989**, *93*, 495.
(16) Guinier, A. *X-ray Diffraction in Crystals, Imperfect Crystals and Amorphous Bodies*; W. H. Freeman: San Francisco, 1963.
(17) Wang, Z. H.; Li, C.; Scherr, E. M.; MacDiarmid, A. G.; Epstein, A. J. *Phys. Rev. Lett.* **1991**, *66*, 1745.
(18) Javadi, H. H. S.; Chakraborty, A.; Li, C.; Theophilou, N.; Swanson, D. B.; MacDiarmid, A. G.; Epstein, A. J. *Phys. Rev. B* **1991**, *43*, 2183.
(19) Epstein, A. J.; MacDiarmid, A. G.; Pouget, J. P. *Phys. Rev. Lett.* **1990**, *65*, 664.

**Registry No.** POT-ES, 135506-25-1.